BeBeC-2018-D16

DEVELOPMENT OF BEAMFORMING METHODS FOR UNCORRELATED DIPOLE SOURCES

Matvey Demyanov[1,2], Oleg Bychkov[1,2], Georgy Faranosov[1,3], Mikhail Zaytsev[1,3]
[1]Central Aerohydrodynamic Institute (TsAGI)
17 Radio str., 105005, Moscow, Russia
[2]Moscow Institute of Physics and Technology
9 Institutskiy per, 141701, Dolgoprudny, Russia
[3]Perm National Research Polytechnic University
29 Komsomolskiy pr., 614990, Perm, Russia

ABSTRACT

Conventional beamforming (CB) algorithm was realized and then generalized for dipole-type sources that makes possible to obtain acoustic maps of dipole moments. The algorithms were exposed to verification and experimental validation in TsAGI acoustic chamber AC-2 for three sound sources: simple tonal beeper, noise from a cylinder streamlined by a jet flow, and jet-plate interaction noise. Azimuthal decomposition technique (ADT) was used to validate dipole-based algorithm. The results obtained demonstrate that, in certain cases, adaptation of the beamformer algorithm to the source features is necessary for its correct localization.

1 INTRODUCTION

In the last decades, multichannel systems for noise source localization become popular since they allow extracting much more information on the sound field compared to standard one-point measurements. The most commonly used method of source localization is based on plane microphone arrays – the so-called “Beamforming” [1-6]. The term “Beamforming” refers to the methods of the localization of noise source position and its acoustic power by means of special postprocessing of acoustic pressure data synchronously recorded by an array of microphones. As applied to aeroacoustics, localization of the noisiest flow domains should help in development of purposive noise reduction methods.

Nowadays, beamforming algorithms are realized as standard tools in commercial data postprocessing software. These algorithms are usually based on a representation of the sound field via a linear combination of uncorrelated monopoles [2]. However, application of such methods may sometimes require modifications to adjust them to the specific experimental conditions (e.g. presence of co-flow, shear layer refraction, multipole noise sources etc.), otherwise source localization and its power determination may be incorrect [1,7,8]. This

means that the users of beamforming arrays should have an opportunity to adapt postprocessing procedure depending on the problem.

In TsAGI, for beamforming measurements, a 42-channel Bruel&Kjaer antenna is used with standard Bruel&Kjaer software [9]. Recently, we decided to develop in-house postprocessing tools in order to have possibility of algorithm adaptation to the source properties. In the current paper, we present in-house beamforming algorithms: one based on the monopole-type steering vectors and the other – on the dipole-type steering vectors (generally similar to that described in [7]). The algorithms were exposed to verification and experimental validation in TsAGI acoustic chamber AC-2 for three types of sound sources: simple tonal beeper, noise generated by a cylinder streamlined by a jet flow, and jet-plate interaction noise.

In the latter two cases, dipole noise can dominate at low and moderate frequencies. For validation purposes, azimuthal decomposition technique (ADT) was used. This method is intensively used at TsAGI as noise sources diagnostic tool. It was successfully applied to identify the sources of vortex ring noise [10], jet noise [11,12], bluff body noise [13], jet-plate interaction noise [14]. This method requires azimuthal array of microphones and has quite high accuracy and resolution. It also allows extracting different multipole components of the sound field and judge about noise generation mechanisms. Thus, ADT suits well for beamforming methods validation on basis of the well-known multipole sources. Note also that in some cases it is problematic to use azimuthal arrays (e.g. at large-scale test rigs [12] or for very complex source structures), and then application of plane beamforming arrays may become more convenient.

2 MONOPOLE AND DIPOLE BEAMFORMING ALGORITHMS

2.1 Algorithm description

Conventional beamforming (CB) method was initially realized in a standard way – on basis of monopole sources, and then modified for incoherent acoustic dipoles (similar approach was realized in [7]). We assume that the sources to be localized lie in the *xy*-plane, and that the microphone array plane is parallel to *xy*-plane. According to CB algorithm, pressure induced on the microphone array is expressed using steering vectors:

$$p_i = \sum_{j=1}^{N_s} \left(a_{xj} q_{xj} + a_{yj} q_{yj} \right), \tag{1}$$

where a_{xj}, a_{yj} – amplitudes of *x* and *y*-dipoles located at *j*-position in the sources mesh; q_{xj}, q_{yj} – steering vectors for these dipoles, that physically correspond to pressures induced by a unit dipole on the microphone array; p_i – pressure on *i*-microphone in the array; N_s – number of nodes in the sources mesh.

Assuming that the sources *x* and *y*- dipoles are incoherent, cross-spectral matrix (CSM) has the form $CSM_{ij} = \overline{p_i p_j^*} = \sum_{k=1}^{N_s} \overline{a_{xk}^2} q_{xk} q_{xk}^H + \overline{a_{yk}^2} q_{yk} q_{yk}^H$. Thereby, similarly to CB, optimization procedure for determination of $A_k = \overline{a_{xk}^2}$, $B_k = \overline{a_{yk}^2}$ consists in the following minimization $\left\| CSM - A_k q_{xk} q_{xk}^H - B_k q_{yk} q_{yk}^H \right\| \xrightarrow[A,B]{} \min$, where A_k, B_k – powers of *x* and *y*-dipoles in *k* position; CSM – matrix constructed from experimental data.

The solution of the minimization problem is:

$$A_k = \frac{\|q_{yk}\|^4 \, q_{xk}{}^H CSMq_{xk}{}^H - \|q_{xk}{}^H q_{yk}\|^2 \, q_{yk}{}^H CSMq_{yk}{}^H}{\|q_{xk}\|^4 \|q_{yk}\|^4 - \|q_{xk}{}^H q_{yk}\|^4},$$
$$B_k = \frac{\|q_{xk}\|^4 \, q_{yk}{}^H CSMq_{yk}{}^H - \|q_{xk}{}^H q_{yk}\|^2 \, q_{xk}{}^H CSMq_{xk}{}^H}{\|q_{xk}\|^4 \|q_{yk}\|^4 - \|q_{xk}{}^H q_{yk}\|^4}. \quad (2)$$

Thus, the described algorithm allows localization of uncorrelated dipole sources. Note that if we assume that the x and y-dipoles at each point of the sources mesh are correlated (in this case, the resulting dipole moment will be inclined at the angle $\arctan(a_{yj} / a_{xj})$ to the x-axis), the minimization problem should be solved in iterative way. However, our tests showed that even uncorrelated approach can give good approximation of the dipole amplitude and its orientation for such correlated dipole components. In the current paper, we use simple algorithm with uncorrelated x and y-dipoles.

2.2 Algorithms verification

Firstly, we verify the basic monopole-based CB algorithm. Virtual microphone array consists of 42 microphones located at the same positions as in the Bruel&Kjaer array used at TsAGI (Fig. 1a). Three point time-harmonic monopole sources of comparable amplitudes were located in the focal plane of the array. Localization results are shown in Fig. 1b. The positions and the amplitudes of the sources were correctly determined. DAMAS and CLEAN-PSF algorithms were also realized for monopole-type steering vectors, however their verification results are not given because hereafter only CB method, realized both for monopoles and dipoles, will be used.

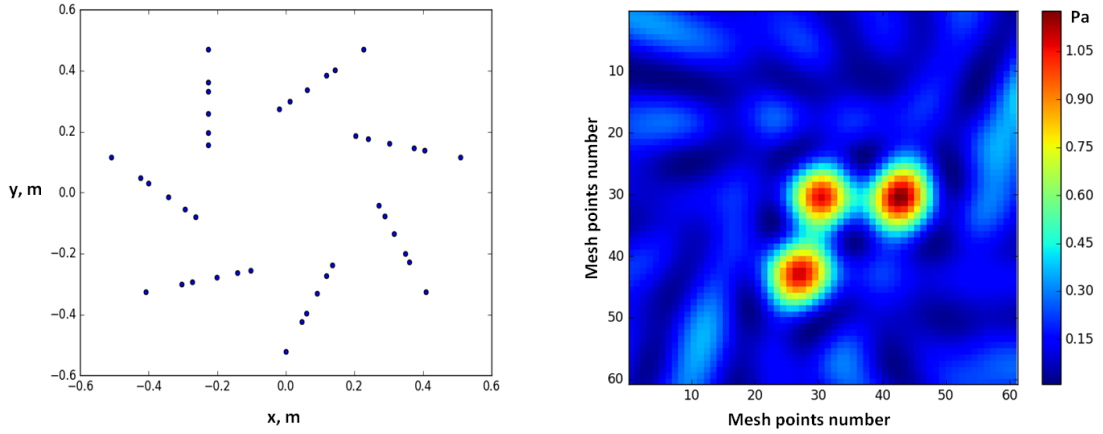

a *b*

Fig. 1. Monopole sources localization (frequency 3 kHz): (a) – microphones positions; (b) – source map (linear scale).

Then, localization of dipole source was considered. The dipole moment of the virtual source was oriented along the y-axis, parallel to the array plane (as shown in [7], in case when the dipole moment is orthogonal to the array plane, monopole algorithm works well). The

results of the application of the standard monopole-based CB algorithm are presented in Fig. 2a. Two intensity peaks are seen on the source map for this case (similar result was obtained in [7]). The central point between the peaks approximately corresponds to the dipole position (specified as {0, –0.2}), however the amplitudes of these peaks are much less than the amplitude of the simulated dipole.

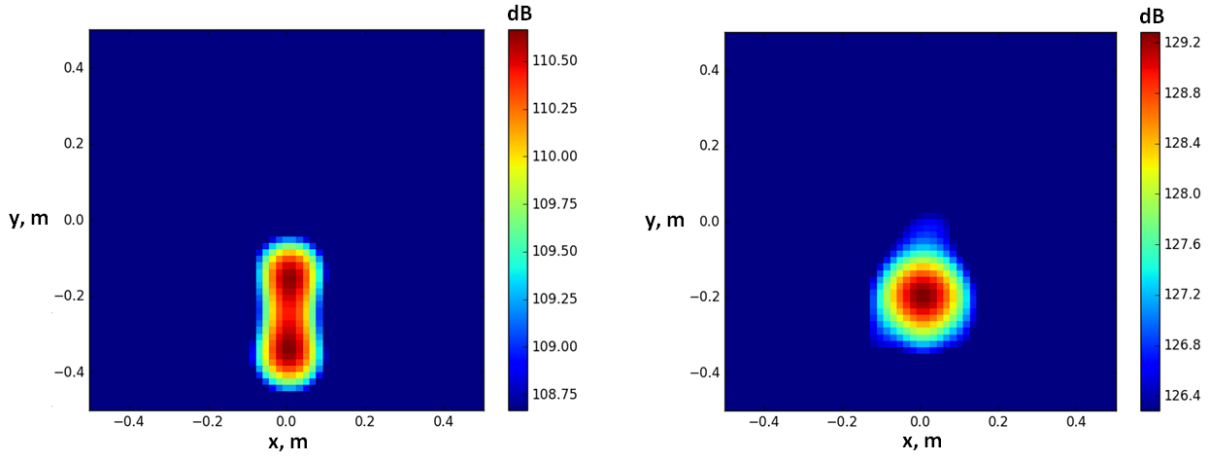

a *b*

Fig. 2. Dipole source localization results (frequency 3 kHz): (a) – by the monopole-based algorithm; (b) – by the dipole-based algorithm.

If it is unclear beforehand what type of source (monopole or dipole) we deal with, the source map in Fig. 2a can be erroneously interpreted as a combination of the two uncorrelated monopoles. Thus, the monopole-based algorithm cannot provide reliable source localization and source amplitude assessment for the dipole source with dipole moment parallel to the array plane. On the contrary, application of the dipole-based algorithm allows correct source localization and gives correct values for the source amplitude (Fig. 2b).

3 VALIDATION OF THE ALGORITHMS

3.1 Test rig

Experiments were carried out in TsAGI anechoic chamber AC-2 designed for aeroacoustic measurements. The dimensions of the free space in the facility (with acoustic wedges on the walls) are 9.54×5.28×4.20 m^3.

The sound-absorbing lining of the anechoic facility consists of wedges filled with Capron fibre and covered with Capron cloth AIT and additional fibreglass cloth. The operating frequency range f of the AC-2 is $f > 200$ Hz for which the reflection coefficient at normal incidence β of the sound-absorbing construction is $\beta \leq 0.1$.

The airflow into the anechoic facility is supplied by a system of gasholders and a fan into three coaxial ducts thus providing the possibility to simulate single- and double-stream jets in static and flight conditions. The air-supplying ducts are equipped with mufflers and de-turbulizing mesh screens, which are designed for suppressing pressure and velocity pulsations (Fig. 3). For the present investigations, a small-scale single-stream nozzle, of diameter D=40 mm, was used (see details below).

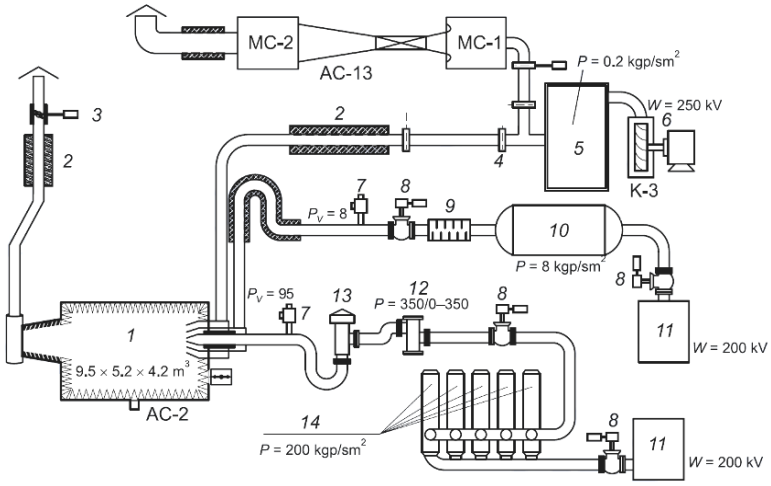

Fig. 3. Sketch of TsAGI aeroacoustic facility: 1 – anechoic chamber, 2 – sound attenuation panel, 3 – heating valve, 4 – damper, 5 – prechamber, 6 – electric motor, 7 – emergency valve, 8 – valve, 9 – filter, 10 – receiver, 11 – compressor, 12 – pressure reducer, 13 – cutoff valve, 14 – gasholders.

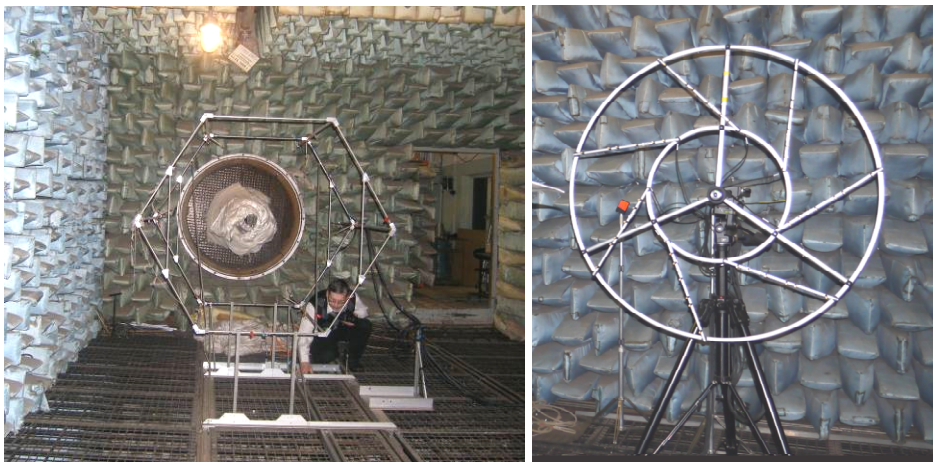

a *b*

Fig. 4. Microphone arrays used in the experiments: (a) – ADT array; (b) – beamforming array.

3.2 Microphone arrays

In the tests, we used two types of microphone arrays: ADT array (Fig. 4a) and beamforming antenna (Fig. 4b). Beamforming measurements were performed by 42-channel Bruel&Kjaer array of 1 m diameter with working frequency range ~0.3…6.4 kHz.

ADT is realized in TsAGI anechoic chamber AC-2 as a standard tool to study noise generated by turbulent flows [11,12]. Noise modal structure is measured by means of a circular array, of diameter 1.5-1.7 m, with (normally) 6 microphones providing good modal resolution up to azimuthal mode n=2 for low and moderate frequencies (up to 3-4 kHz depending on the problem) [10-15]. The array can be shifted step-by-step along the chamber, the microphones moving along the six corresponding generatrices of the cylindrical surface enclosing the noise source. Microphone array movement is controlled by the automatic

traverse system FESTO. Azimuthal decomposition procedure is realized on basis of multi-channel Bruel&Kjaer analyzer platform, and in-house code for the azimuthal modes calculation. In the current experiments, simplified two-microphone version of ADT was used [15] because we were interested in the cases with dipole source domination, and thus two microphones were enough to extract required noise components.

3.3 Simple time-harmonic source

At the first step of the basic algorithm validation, a simple time-harmonic source was considered. The source (beeper) operated at frequency 2.5 kHz. The array was located at a distance R=1.5 m from the source (Fig. 5). Localization was performed by means of the standard monopole-based algorithm. The results of the source localization obtained by Bruel&Kjaer software (Refined Beamforming) and in-house tool are shown in Fig. 6. In Fig. 6 and in the subsequent figures, sound pressure levels on the source maps are scaled to the distance 1 m from the source.

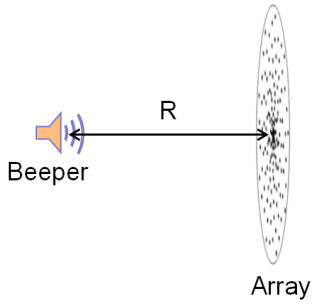

Fig. 5. Sketch of the experiment with time-harmonic source.

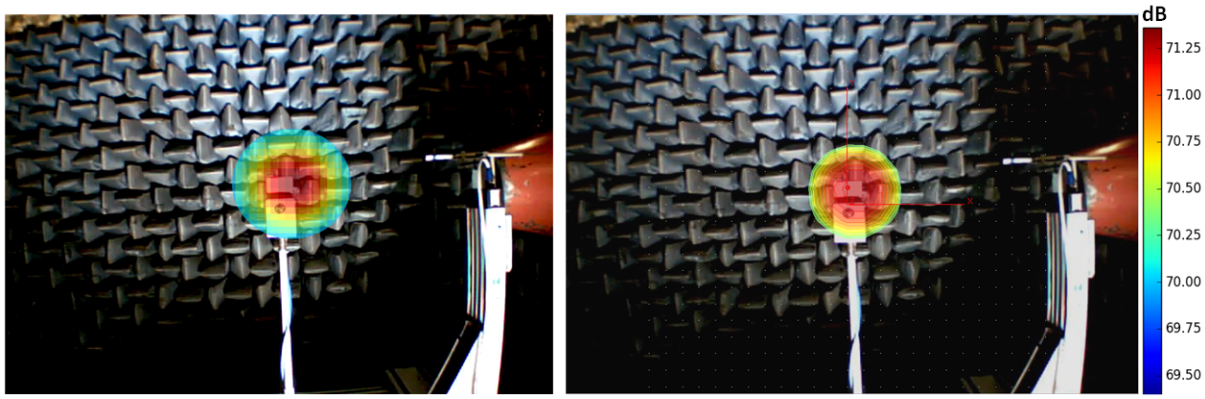

a *b*

Fig. 6. Time-harmonic source localization in anechoic chamber AC-2 (frequency 2.5 kHz): (a) – in-house CB algorithm; (b) – Bruel&Kjaer software.

3.4 Cylinder streamlined by a jet

One of the typical configurations where dipole noise sources arise is a bluff body streamlined by a flow [7,13,16]. In our series of experiments, noise was generated by a cylinder, 5 mm diameter, inserted into turbulent jet issued from 40 mm round nozzle. Jet velocity was 100 m/s, the cylinder was located 250 mm downstream from the nozzle exit

(Fig. 7d). The cylinder could be rotated around the jet axis so that different orientations were investigated (Fig. 7c).

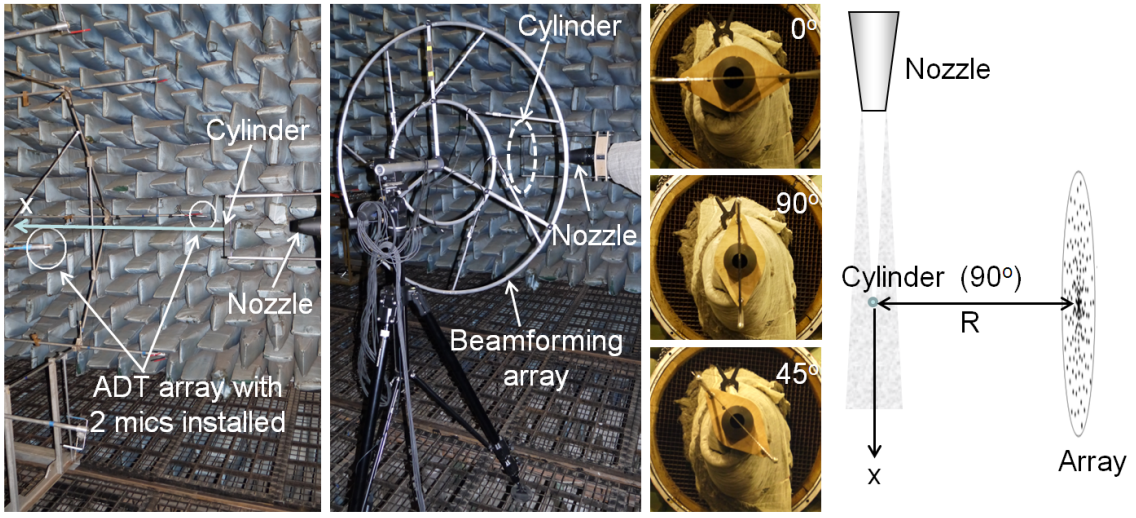

a *b* *c* *d*

Fig. 7. Experiments with bluff-body noise: (a) – ADT microphone array; (b) – beamforming microphone array; (c) – cylinder orientations; (d) – sketch of the beamforming experiment.

Azimuthal structure of cylinder noise was investigated in detail in [13]. It was shown that drag and lift dipoles (x- and y-ones) generate much more noise compared to viscous z-dipole. Thus, only two microphones in the ADT array (Fig. 7a) are enough to recover all significant azimuthal modes (axisymmetric one and the first, antisymmetric, one):

$$p(x,\theta,R_a,t) \approx a_0(x,R_a,t) + a_1(x,R_a,t)\cos\theta + \dots, \tag{3}$$

where (x,θ,r) – cylindrical coordinates, $R_a = 0.75$ m – array radius. If the two opposite microphones are located as shown in Fig. 9a, then modal time histories can be assessed as

$$\begin{aligned} a_0(x,R_a,t) &\approx \big(p(x,0,R_a,t) + p(x,\pi,R_a,t)\big)/2, \\ a_1(x,R_a,t) &\approx \big(p(x,0,R_a,t) - p(x,\pi,R_a,t)\big)/2. \end{aligned} \tag{4}$$

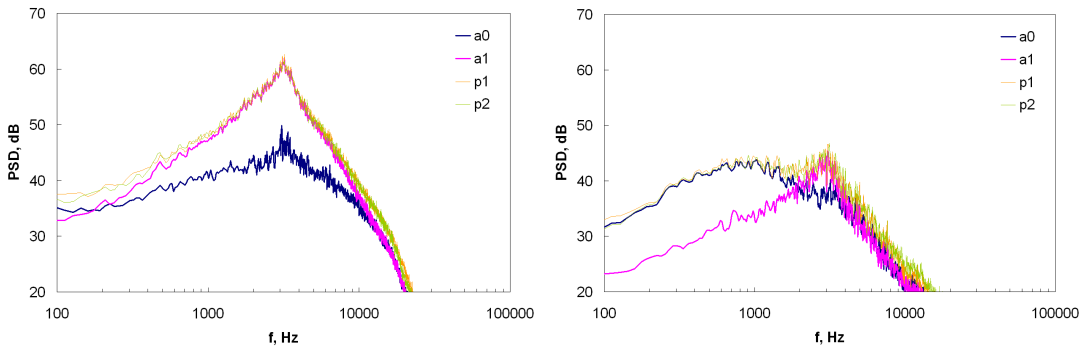

a *b*

Fig. 8. Spectra of raw signals and azimuthal modes for different ADT array positions: (a) – x=0 (corresponds to the cylinder location); (b) – x=1.3 m.

Coordinate of the ADT array was varied in the range x={-0.5 m,…, 1.3 m}, x=0 corresponded to the cylinder location (Fig. 7). Spectra of raw signals and azimuthal modes for different ADT array positions are shown in Fig. 8. It is seen that lift dipole (mode a_1) dominates the sound field around spectral maximum. For large x (shallow angles to the jet axis), it can be seen significant contribution of jet noise into the total signal. This jet contribution is axisymmetric (mode a_0, see [11,12,15]) and thus antisymmetric dipole component a_1 can be easily recovered by the two-microphone system.

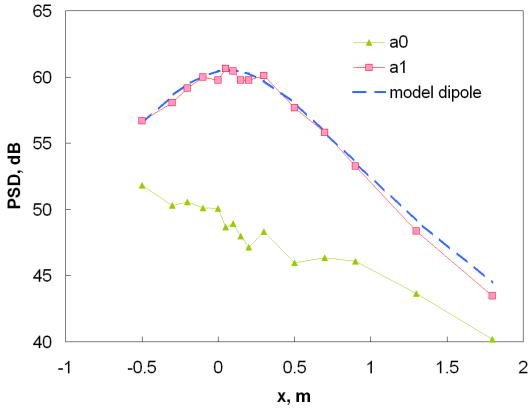

Fig. 9. Distribution of the azimuthal modes intensities on the cylindrical surface surrounding the source, frequency band 2.9-3.1 kHz (around the peak in the noise spectrum). Dashed line corresponds to the point dipole of 81 dB intensity.

The distribution of the azimuthal modes intensities on the cylindrical surface surrounding the source is shown in Fig. 9 for the frequency band 2.9-3.1 kHz (around the peak in the noise spectrum). Also shown is the model curve representing point dipole located at x_0=0.07 m, with the intensity corresponding to L=81 dB with PSD level defined as:

$$PSD(x) = \frac{4 \cdot 10^{L/10-10}}{\Delta f} \frac{R_a^2}{\left(R_a^2 + (x - x_0)^2\right)^2}, \tag{5}$$

where Δf =0.2 kHz is the width of the analysed frequency range.

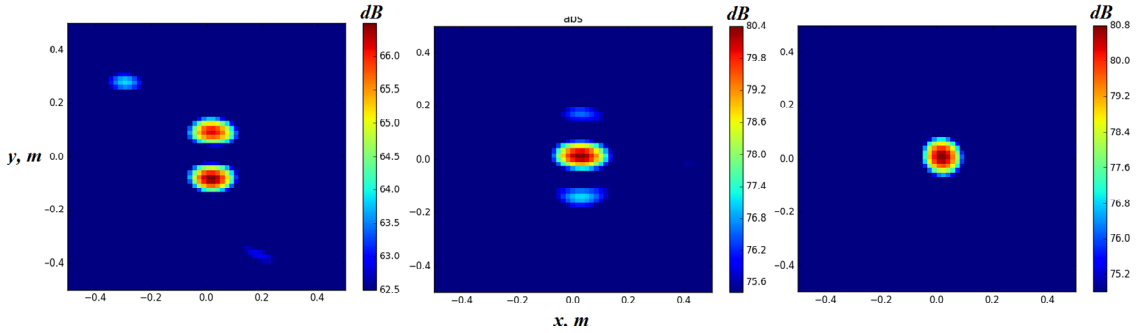

a *b* *c*

Fig. 10. Localization of noise sources by means of: (a) beamforming with the standard monopole-based algorithm, cylinder orientation 0^0; (b) beamforming with the modified dipole algorithm, cylinder orientation 0^0; and (c) beamforming with standard monopole-based algorithm, cylinder orientation 90^0.

Beamforming localization results are shown in Fig. 10 for different algorithms and cylinder orientations. As for model situation described in section 2.2, monopole-based algorithm gives incorrect localization and source power assessment when the dipole moment is parallel to the array plane (Fig. 10a). Dipole-based algorithm allows reconstructing both the source position and its amplitude (Fig. 10b). However, when the cylinder is oriented so that the lift dipole's maximum radiation lobe is directed towards the array center (90^0 cylinder orientation according to Fig. 7), monopole algorithm again works well (Fig. 10c). This is because the part of the radiation incident on the array is close to omnidirectional and has no phase jump by 180^0 like in the previous 0^0 orientation.

3.5 Jet-plate interaction noise

Another case where dipole-type noise sources can play a role is the one connected with the jet installation noise. It is known (e.g. see [14]) that the jet located close to the wing radiates much more noise compared to uninstalled configuration. In the current work, simple jet-plate system was investigated again both by means of ADT array and beamforming antenna. The plate was installed parallel to the jet axis as shown in the sketch in Fig. 11 with the parameters d=3.15D, h=D, D=40 mm – is the nozzle diameter. Acoustic Mach number of the jet was 0.4.

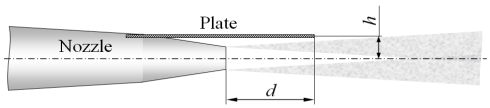

Fig. 11. Jet-plate configuration.

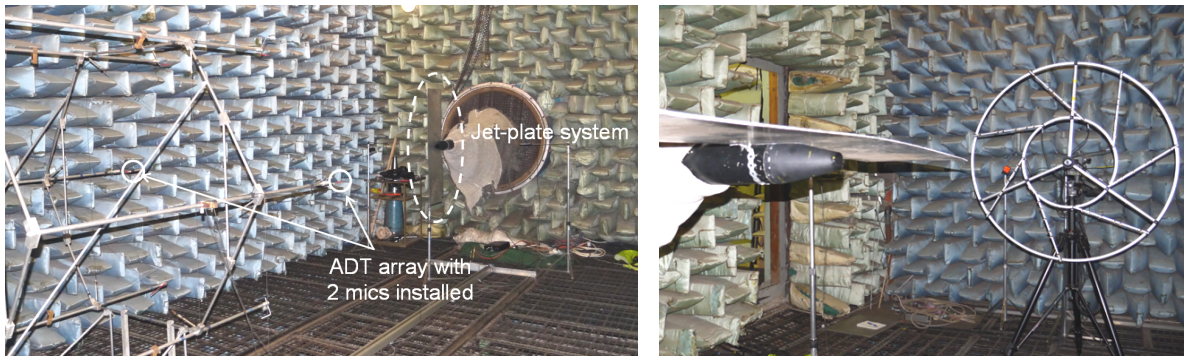

a *b*

Fig. 12. (a) ADT and (b) beamforming measurements of the jet-plate configuration.

Again, for simplicity, two-microphone ADT was used. The plate was oriented vertically as shown in Fig. 12. Coordinate of the ADT array was varied in the range x={-0.5 m,…, 2.5 m}, x=0 corresponded to the nozzle exit (Fig. 12). As shown in [14,15], at sideline directions antisymmetric mode a_1 dominates the total noise at low frequencies, while for shallow angles jet noise mode a_0 becomes comparable to a_1. This effect is demonstrated in Fig. 13 where the spectra of the symmetric and antisymmetric azimuthal modes are presented for different ADT array positions. The modes were defined in accordance with Eqs. (4).

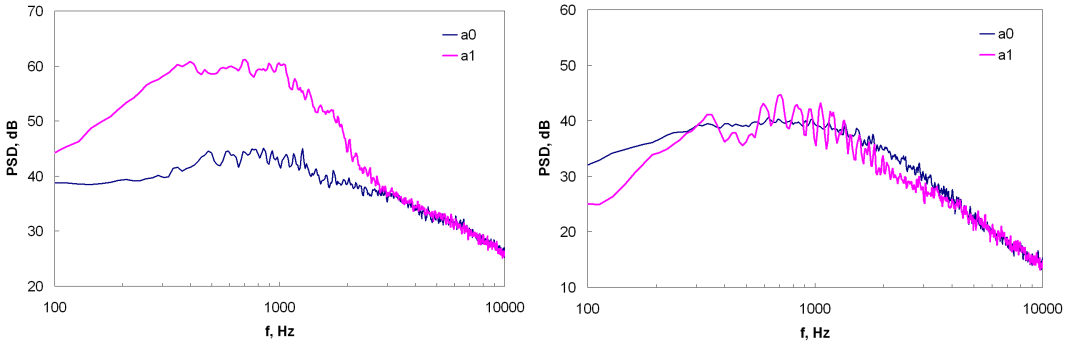

Fig. 13. Spectra of the symmetric and antisymmetric azimuthal modes for different ADT array positions: (a) – x=0 (corresponds to the nozzle exit); (b) – x=2.5 m.

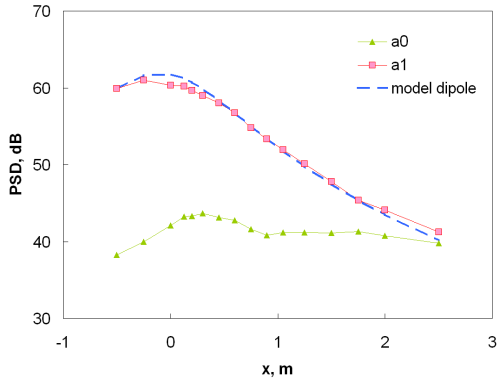

Fig. 14. Distribution of the azimuthal modes intensities on the cylindrical surface surrounding the source, frequency band 0.5-0.7 kHz. Dashed line corresponds to the point dipole of 83 dB intensity.

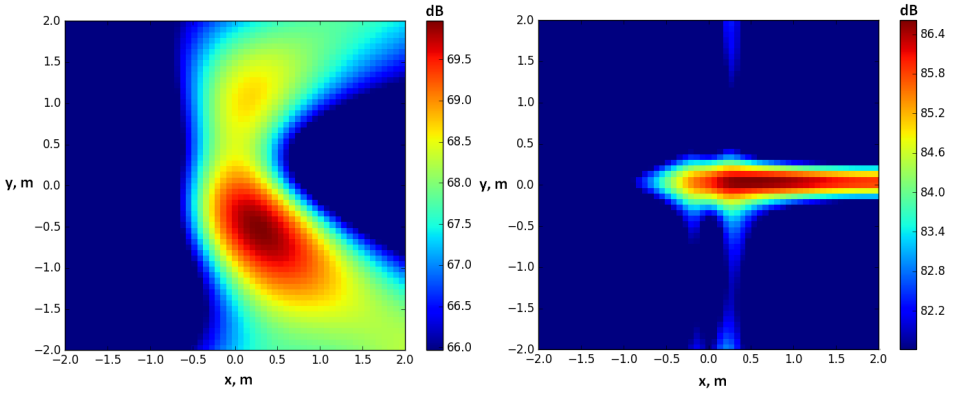

a *b*

Fig. 15. Beamforming localization of the noise sources by means of: (a) monopole-based algorithm; (b) modified dipole algorithm.

The distribution of the azimuthal modes intensities on the cylindrical surface surrounding the jet is shown in Fig. 14 for the frequency range 0.5-0.7 kHz. Also shown is the model curve representing point dipole with the intensity corresponding to L=83 dB. The model curve was calculated in accordance with Eq. (5).

Beamforming results are presented in Fig. 15. Generally, the results are similar to those obtained for cylinder noise in section 3.4. Again, for the dipole source with the moment coplanar to the array plane, the monopole-based algorithm gives incorrect localization and power assessment (Fig. 15a), while modified dipole-based method recovers adequate source position and amplitude (Fig. 15b), however, in contrast to cylinder noise, there is 3 dB difference between ADT and beamforming data for jet-plate noise. This can be related to the fact that in the latter case the scattered field is not a pure dipole [14] and the performance of the dipole algorithm may require more careful analysis.

4 CONCLUSIONS

Conventional beamforming algorithm was realized as in-house tool and then generalized for dipole-type sources that makes possible to obtain acoustic maps of dipole moments. The algorithms were verified using virtual point sources and validated in TsAGI acoustic chamber AC-2 for three types of sound sources: simple tonal beeper, noise from a cylinder streamlined by a jet flow, and jet-plate interaction noise. For the latter two cases, validation was performed by means of ADT results obtained for the same sources.

It is shown that application of dipole-based beamforming algorithm may improve source localization when dipole sources play a role in the sound field and is oriented in such a way that the dipole moment is coplanar to the array plane. It should be noted that the localization of the considered sources by means of ADT usually provides higher accuracy and does not require a priori knowledge of the source orientation provided the source is compact and centered at the array axis and the number of microphones is sufficient. However, ADT is not suitable for complex sources, e.g. for noise produced by real aircraft (with contributions from engines, flaps, slats, landing gear, cavities, struts etc.) – only beamforming antennas may provide adequate localization in such cases.

Generally, the results obtained demonstrate that, in certain cases, adaptation of the beamformer algorithm to the source features is necessary for its correct localization. Moreover, it seems that comparative study of different beamforming algorithms may provide indirect evidence on the true structure of the sound field that can be used to clarify noise source physics.

ACKNOWLEDGMENTS

The authors are grateful to Professor Victor Kopiev for helpful discussions and continuous interest to this work.

The work was partially supported by the Russian Ministry of Education and Science under the grant 14.Z50.31.0032 (development of the beamforming algorithms), by the Russian Foundation for Basic Research under the grant 16-01-00746a (experiments with cylinder), and by the Russian Ministry of Industry and Trade, project “ORINOCO-2” (experiments with jet-plate interaction).

REFERENCES

[1] J. Billingsley, R. Kinns. “The acoustic telescope.” J. Sound Vib., 48, 485-510, 1976.

[2] B. Dougherty. “Phased Array Technology Applied to Aeroacoustics.” In Keynote Lecture 15th AIAA/CEAS Aeroacoustics Conference, Miami, Florida, USA, 11-13 May 2009.

[3] J. Piet, U. Michel, P. Bohning. "Localization of the Acoustic Sources of the A340 with A Large Phased Microphone Array During Flight Tests." AIAA-2002-2506, 2002. 8th AIAA/CEAS Aeroacoustics Conference, Breckenridge, Co, 17-19 June 2002.

[4] P. Sijtsma. "CLEAN based on spatial source coherence." AIAA-2007-3436, 2007. 13th AIAA/CEAS Aeroacoustics Conference, Rome, Italy, 21-23 May 2007.

[5] V. Fleury, R. Davy. "Analysis of jet-airfoil interaction noise sources by using a microphone array technique." J. Sound Vib., 364, 44-66, 2016. doi: 10.1016/j.jsv.2015.11.027.

[6] U. Michel, B. Barsikow, J. Helbig. M. Hellmig, M. Schuettpelz. "Flyover noise measurements on a landing aircraft with a microphone array." AIAA-98-2336, 1998. 4th AIAA/CEAS Aeroacoustics Conference, Toulouse, France, 2-4 June 1998.

[7] Y. Liu, A. Quayle, A. Dowling. "Beamforming correction for dipole measurement using two-dimensional microphone arrays." JASA, 124, 182-191, 2008. doi: 10.1121/1.2931950

[8] R. Porteous, Z. Prime, C. Doolan, D. Moreau, V. Valeau "Three-dimensional beamforming of dipolar aeroacoustic sources." J. Sound Vib., 355, 117-134, 2015. doi: 10.1016/j.jsv.2015.06.030.

[9] V. Kopiev, M. Zaytsev. "Application of beamforming to jet/flap interaction noise." BeBeC-2014-24, 2014. 5th Berlin Beamforming Conference, 19-20 February, 2014.

[10] V. Kopiev, M. Zaytsev, S. Chernyshev. "Sound radiation from a free vortex ring and a ring crossing an obstacle," AIAA-1998-2371, 1998. 4th AIAA/CEAS Aeroacoustics Conference, Toulouse, France, 2-4 June 1998.

[11] V. Kopiev. "Azimuthal decomposition of turbulent jet noise and its role for diagnostic of noise sources." VKI Lecture Series 2003-04 "Advances in Aeroacoustics and Applications", 2003.

[12] G. Faranosov, I. Belyaev, V. Kopiev, M. Zaytsev, A. Aleksentsev, Y. Bersenev, V. Chursin, T. Viskova. "Adaptation of the Azimuthal Decomposition Technique to Jet Noise Measurements in Full-Scale Tests." AIAA Journal, 55(2), 572-584, 2017. doi: 10.2514/1.J055001.

[13] M. Zaitsev, V. Kopiev. "Mechanism of sound radiation by turbulence near the rigid body," Fluid Dynamics, Vol. 43, No. 1, 2008, pp. 98–109. doi: 10.1134/S0015462808010109

[14] G. Faranosov, V. Kopiev, I. Belyaev, O. Bychkov, S. Chernyshev. "On the Azimuthal Structure of Installed Jet Noise," AIAA-2017-3527, 2017. 23rd AIAA/CEAS Aeroacoustics Conference (2017 AIAA AVIATION Forum), Denver, Co, 5-9 June 2017.

[15] V. Kopiev, G. Faranosov, I. Belyaev, M. Zaytsev. "Development of experimental method for azimuthal mode measurement for jet-wing interaction noise." 24th International Congress on Sound and Vibration, ICSV 2017, London, United Kingdom, 23-27 July 2017.

[16] N. Curle. "The Influence of Solid Boundaries on Aerodynamic Sound." Proc. R. Soc. London. Ser., A 231, No. 1187, 1955, pp. 505-514.